

## Swirling Performance of Rotational Mixing Vane in Subchannel using CFD

Han Eol Park, Han Seo, In Cheol Bang\*  
Department of Nuclear Engineering  
Ulsan National Institute of Science and Technology (UNIST)  
50 UNIST-gil, Ulju-gun, Ulsan, 44919, Republic of Korea  
\*Corresponding author: icbang@unist.ac.kr

### 1. Introduction

There are numerous studies related to the analysis of swirl performance in subchannel conditions to enhance the heat transfer performance as well as critical heat flux (CHF). Recently, Seo et al. [1] compared swirl performance using three types of vanes in vertical and horizontal square duct: (1) spacer grid (SG), (2) fixed split vane (FSV), and (3) moving rotational vane (MRV). Particle image velocimetry (PIV) technique was used to measure the flow distributions at the downstream of the test section to evaluate the mixing effect with three types of the vanes. In addition, computational fluid dynamic (CFD) analysis was performed to simulate the swirl generation of the mixing vane. Commercial available CFD code, FLOW-3D, was used to show the swirling effect of MRV in the flow channel. But, there was a discrepancy between the experimental and the simulation results in the condition of the MRV due to the different rotational speed of the vane.

In the present study, the same design of the MRV was used by changing CFD analysis conditions: the MRV was suggested as fixed solid. The evaluation of the swirling performance with non-moving rotational vane (NMRV) is needed to determine the inherent design characteristics of the MRV. Therefore, the analysis with the NMRV can provide the physical practicality of the rotating vane (RV).

### 2. CFD Modeling

#### 2.1. Vane Design

Fig. 1 exhibits the shape of the SG, FSV, and RV for the CFD analysis: NMRV has same structural grid compared to the MRV. To analyze different temporal conditions of rotational vane, two NMRV models were considered: one has same angle of rotational vane with time at 0, the other rotated 45° from that model. Each simulation condition was named as NMRV1 and NMRV2, respectively.

To demonstrate the effect of the MRV, comparing group SG, FSV, and MRV is designed. SG is wall with 3 mm thickness, has a length of 147mm. The FSV vanes are depicted as 30°angle relative to the flow direction, 19mm and 15.2 mm width is applied. They configured a similar shape to that commonly

used in nuclear power plants. On the other hand, the rotational vane model is based on a patent [3], with four blades. The angle of the rotational vane is same as the FSV. Three types of the vanes were used in the CFD analysis for the comparison of the mixing effects.

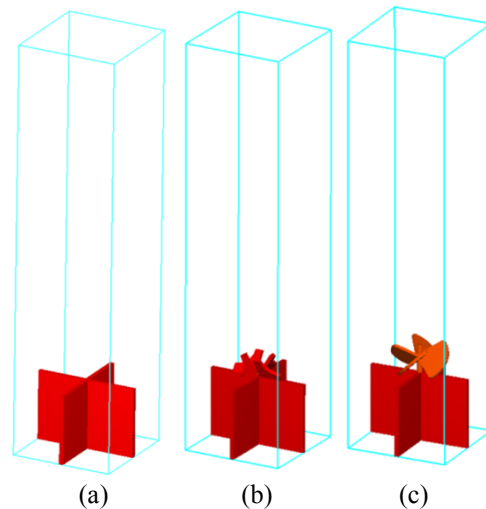


Fig. 1. CFD structure of vanes (a) SG, (b) FSV, (c) RV

#### 2.2. Flow-3D analysis

In this study, flow channel was designed as the same condition reported by the previous study [1]. The length and the width of the flow channel are 300mm and 68mm, respectively. RNG  $k-\epsilon$  model was used for modeling of inhomogeneous turbulent flow. The initial flow speed is 0.8 m/s. The relative outlet pressure was 0 Pa to calculate the pressure drop. To obtain particle visualization, air bubble injection simulation was considered with 4 sources at the upstream of the test section. The air bubble was assumed as density of 1 kg/m<sup>3</sup> with the diameter of 0.002 m.

For the analysis of general moving object(GMO) model, volume of fluid (VOF) transport equation is used through flow-3D. The hydraulic force and torque due to pressure and shear stress are added in coupled motion, so equations of motion are solved for the moving objects under coupled motion. The moving object is updated each time step, based on the applied force based on the continuity equation and the VOF transport equation:

$$\frac{V_f}{\rho} \frac{\partial \rho}{\partial t} + \frac{1}{\rho} \nabla \cdot (\rho \vec{u} A_f) = -\frac{V_f}{dt} \quad (1)$$

$$\frac{\partial F}{\partial t} + \frac{1}{V_f} \nabla \cdot (F \vec{u} A_f) = -\frac{F}{V_f} \frac{\partial V_f}{\partial t} \quad (2)$$

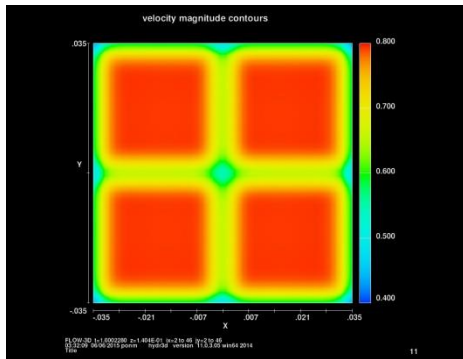
Where  $V_f$  is the volume fraction,  $\rho$  is the fluid density,  $t$  is the time,  $\vec{u}$  is the fluid velocity,  $A_f$  is the area fraction, and  $F$  is the fluid fraction [4]. However, instead of MRV, including NMRV, GMO model is not activated.

### 3. Results and discussion

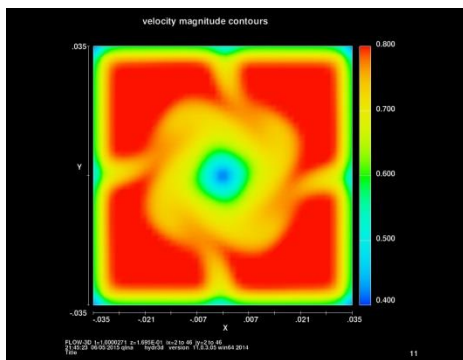
#### 3.1 Visualization of flow distributions

Fig. 2 exhibits cross section velocity fields at 100mm from the each vane. Colored contour is velocity magnitude of SG, FSV, MRV, and NMRV is shown relatively.

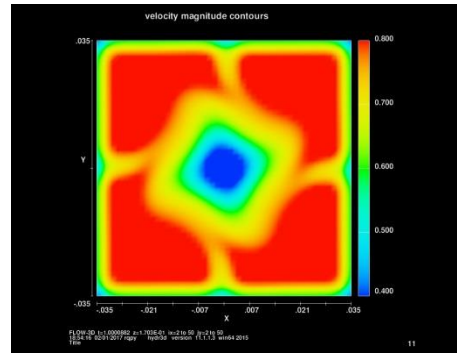
As shown in Fig. 2, the MRV and NMRV show the enhanced swirling performance, comparing to the SG and FSV. For SG, no turbulent flow is observed. But velocity difference shows the lateral flow of FSV, MRV, and NMRV.



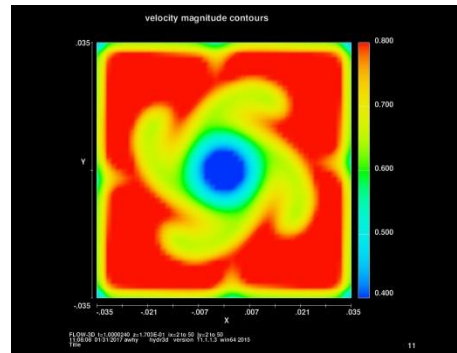
(a)



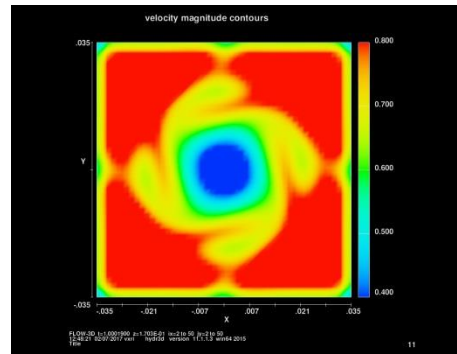
(b)



(c)



(d)



(e)

Fig. 2. Vector magnitude at 100mm from vanes (a) SG (b) FSV (c) MRV (d) NMRV1 (e) NMRV2

#### 3.2 Particle tracking results

Fig. 3 shows simulation the results of the particle tracking method. As shown in Fig. 3(b), air bubble was rotated at the center of the vane due to the swirling effect of FSV. In the Fig. 3, NMRV shows particle swirl generation which tends to make particles to the center of the test section. The swirl generation direction for FSV and NMRV is fixed as 30° angle. On the other hand, MRV shows swirl that makes particle evenly mixed, as rotating. Fig. 3 shows the motion of air bubbles at the center position after passing through the MRV. The swirling flow for MRV and NMRV shows different tendency, however, both model with rotational vane shows particle swirling.

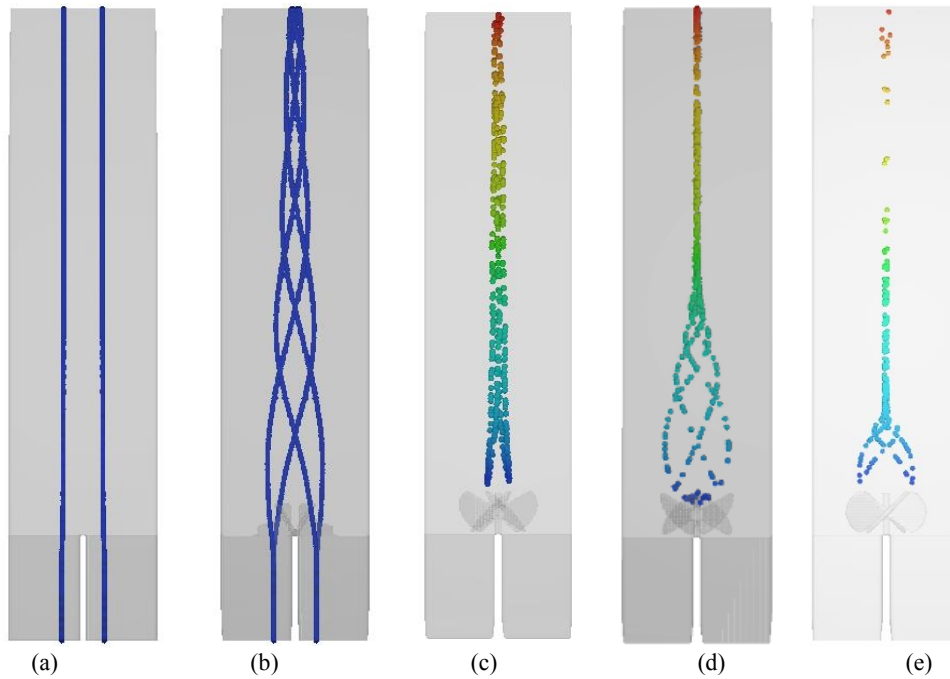


Fig. 3. Particle tracking images (a)SG (b) FSV (c) MRV (d) NMRV1 (e) NMRV2

Seeing Figs 2 and 3, turbulent flow occurs for both MRV and NMRV, with enhanced lateral velocity from SG without vane rotating. Therefore, swirl performance amplified as using the rotational vane.

### 3.3 Swirl ratio

The swirl generation could be described by the swirl ratio. The swirl ratio is defined as the integration of the absolute lateral velocity along the centerline of the lateral direction divided by the axial velocity of the working fluid [1]. Swirl ratio is defined as follows :

$$F_{sw} = \frac{1}{L} \int \frac{|U_{lateral}|}{U_{bulk}} dL \quad (3)$$

Where L is channel width,  $U_{lateral}$  is the swirl velocity, and  $U_{bulk}$  is the streamwise velocity at the measurement sections.  $U_{lateral}$  and  $U_{bulk}$  can be obtained as horizontal and vertical flow, respectively.

Fig. 4 indicates the swirling ratio of each SG, FSV, MRV, and NMRV.

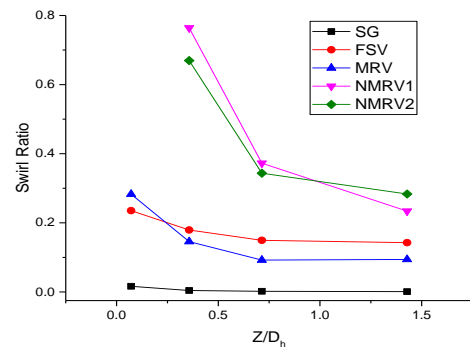


Fig. 4. Swirl ratio graph for each vane

The swirl effect was not observed in the SG, because there was no flow obstacle of the vane. NMRV shows most swirl ratio, scaled as 0.35~0.8. As can be seen in Fig 4, NMRV makes evident swirling effect. MRV shows relatively low swirl ratio comparing with NMRV, almost same as FSV. Still MRV has swirl effect scaled as swirl ratio 0.15~0.28. This difference between NMRV and MRV may due to the GMO model used in the CFD analysis. The GMO model in the CFD analysis, the rotation speed of the RV can be changed as the configuration of the CFD code.

As seen in Figs 2 and 3, both results seem to represent the rotational vane acts as good mixing device. As a result, using the rotational vane in the fuel assembly could bring enhanced turbulent flow for the nuclear subchannel.

#### **4. Conclusion**

Using Flow-3D, CFD analysis was performed for the MRV and NMRV comparing with SG and FSV. The results show the maximum swirl generation and turbulence intensity in NMRV. This means that the RV could provide secondary flow structures such as swirl and cross flow. Rotational vane is investigated to maximize the mixing effect MRV and NMRV models with rotational vane seem to show the improvement on swirling effect of rotating mixing vane.

For the comparison based on swirling effect of mixing vane, change of nonmoving mixing vane, various types of MRV, developed CFD modeling moving mixing vane should be considered for the actual subchannels conditions to investigate swirl and crossflow in the subchannels.

#### **ACKNOWLEDGMENT**

This work was supported by the Nuclear Energy Research Program through the National Research Foundation of Korea (NRF), funded by the Ministry of Science, ICT, and Future Planning (2013M2B2B1075734, NRF-22A20153413555, 2015M2B2A9031869).

#### **REFERENCE**

- [1] H. Seo, S. D. Park, S. B. Seo, H. Heo, I. C. Bang, Swirling performance of flow-driven rotating mixing vane toward critical heat flux enhancement, *International Journal of Heat and Mass Transfer*, 2015.
- [2] Heather L. McClusky, Mary V. Holloway, Donald E. Beasley, Michael E. Conner, Development of swirling flow in a rod bundle subchannel, *Journal of fluids engineering*, 2002.
- [3] I. C. Bang, S. H. Chang, Flow mixing rotation vane attached in nuclear fuel spacer, Korea Patent, No. 10-0456500, 2004.
- [4] Flow science, flow-3D user Manual Version 3.2, 2009.
- [5] S.C.Choi, K.Y.Kim, Numerical analyses of three-dimensional thermo-fluid through mixing vane in a subchannel of nuclear reactor, *Korean Society for Computational Fluids Engineering*, 2002.